Biophysical Chemistry 156 (2011) 79–87

Contents lists available at ScienceDirect

Biophysical Chemistry

journal homepage: http://www.elsevier.com/locate/biophyschem

Understanding the physical basis of the salt dependence of the electrostatic binding free energy of mutated charged ligand–nucleic acid complexes

Robert C. Harris [a], Johan H. Bredenberg [a], Alexander R.J. Silalahi [a], Alexander H. Boschitsch [b], Marcia O. Fenley [a,*]

[a] Department of Physics and Institute of Molecular Biophysics, Florida State University, Tallahasse, FL 32306, USA
[b] Continuum-Dynamics Inc., 34 Lexington Avenue, Ewing, NJ 08618-2302, USA

ARTICLE INFO

Article history:
Received 29 September 2010
Received in revised form 8 February 2011
Accepted 21 February 2011
Available online 9 March 2011

Keywords:
Poisson–Boltzmann equation
Electrostatics
Binding
Counterion condensation theory
Debye–Hückel equation
Generalized Born model

ABSTRACT

The predictions of the derivative of the electrostatic binding free energy of a biomolecular complex, ΔG_{el}, with respect to the logarithm of the 1:1 salt concentration, $d(\Delta G_{el})/d(\ln[NaCl])$, SK, by the Poisson–Boltzmann equation, PBE, are very similar to those of the simpler Debye–Hückel equation, DHE, because the terms in the PBE's predictions of SK that depend on the details of the dielectric interface are small compared to the contributions from long-range electrostatic interactions. These facts allow one to obtain predictions of SK using a simplified charge model along with the DHE that are highly correlated with both the PBE and experimental binding data. The DHE-based model developed here, which was derived from the generalized Born model, explains the lack of correlation between SK and ΔG_{el} in the presence of a dielectric discontinuity, which conflicts with the popular use of this supposed correlation to parse experimental binding free energies into electrostatic and nonelectrostatic components. Moreover, the DHE model also provides a clear justification for the correlations between SK and various empirical quantities, like the number of ion pairs, the ligand charge on the interface, the Coulomb binding free energy, and the product of the charges on the complex's components, but these correlations are weak, questioning their usefulness.

1. Introduction

Given the high negative charge density of nucleic acids, that many charged ligands, including metal cations, cationic drugs, peptides, and large proteins, bind to nucleic acids while carrying out essential biological functions is not surprising. Numerous kinetic and thermodynamic studies have demonstrated that nonspecific electrostatic interactions between the phosphate groups of the nucleic acid and the charged groups of its ligand partner usually cause the binding affinity of these complexes to increase strongly with decreasing salt concentration [1–16]. If competing multivalent ions are not present, the total experimental binding free energy, ΔG, has been observed to vary linearly with the 1:1 salt concentration, [NaCl], and $d(\Delta G)/d(\ln[NaCl])$ is a negative constant, referred to in the literature as SK, at least over a moderate range of salt concentrations [17]. Because SK depends primarily on the nonspecific long-range electrostatic interactions in charged ligand–nucleic acid complexes and is accessible to experimental tests, it has been frequently used to test the predictions of electrostatic theories [18–22].

One of the first methods of successfully predicting SK for a broad range of biopolyelectrolyte complexes was the counterion condensation theory, CCT [17,23]. Its predictions have been confirmed [18,19,24–27] by their agreement with those of the nonlinear Poisson–Boltzmann equation [28,29], NLPBE, which includes features absent in the CCT like a detailed charge distribution and a dielectric discontinuity. However, in our recent study on the binding of small organic drugs to DNA [30], although both the NLPBE and the CCT produce SK predictions that agree with experimental binding data, the NLPBE in the presence of a dielectric discontinuity does not agree with the relation inferred from the CCT, $\Delta G_{el} = -SK\ln[NaCl]$ [31]. This finding is consistent with other PBE studies on RNA-protein systems like TRAP-RNA, tRNA synthetase-tRNA, and aatRNA-elongation factor Tu complex, where small SK did not imply small ΔG_{el} [32–34]. This observation calls into question the common assumption that ΔG_{el} is proportional to SK [31], and indicates that this assumption should not be used to parse experimental binding free energy data into electrostatic and nonelectrostatic components [5,10,15,16,32].

To explain why the predictions of SK by the NLPBE agree with those of the CCT while their predictions of ΔG_{el} disagree in the presence of a dielectric discontinuity, we examined a version of the

* Corresponding author at: Institute of Molecular Biophysics, Florida State University, Tallahassee, FL 32306, USA. Tel.: +1 850 644 7961; fax: +1 850 644 7244.
E-mail addresses: rch02c@fsu.edu (R.C. Harris), johan.h.bredenberg@gmail.com (J.H. Bredenberg), alexandersilalahi@gmail.com (A.R.J. Silalahi), alex@continuum-dynamics.com (A.H. Boschitsch), mfenley@sb.fsu.edu (M.O. Fenley).

0301-4622/$ – see front matter © 2011 Elsevier B.V. All rights reserved.
doi:10.1016/j.bpc.2011.02.010

popular generalized Born [35–37], GB, model. As will be shown later, when the salt derivative of the GB model's prediction of ΔG_{el} is taken and some reasonable approximations are made, the resulting formula for SK is what would be derived from the Debye–Hückel equation, DHE [38]. In our DHE model we assume that the molecules are collections of points charges embedded in a high dielectric solvent region. Thus, there is no dielectric interface separating the low dielectric solute region from the high dielectric solvent region. It should be pointed out that when we refer to the linear Poisson–Boltzmann equation (LPBE) we will be assuming the presence of a dielectric interface between the solute and solvent regions.

In addition, the DHE-based formula here derived also explains the observed correlations between several simple structural or energetic quantities and SK. For example, that SK is roughly proportional to the charge on the ligand for small cations binding to polyelectrolyte nucleic acids is well known, and this proportionality has been verified for numerous biomolecular systems, including multivalent cations, cationic drugs, and oligopeptides binding to polymeric nucleic acids [1,4,10]. This experimental finding agrees with the predictions of both CCT and PBE studies [17,23,26,27,39]. However, the RNA-protein systems investigated in the present study are large and contain a significant number of anionic residues, unlike the complexes in these previous studies. This proportionality between SK and the charge of the ligand would not therefore be expected to hold, and indeed, no correlation can be observed between these two quantities. This finding agrees with the available experimental data on peptides containing anionic residues binding to nucleic acids [15,40–43]. Instead, several other empirical quantities have been proposed to be proportional to SK, including the number of ion pairs [8,44–46], or close ionic contacts between cationic ligand residues and anionic nucleic acid phosphate groups, and, for complexes containing a significant number of anionic residues close to the binding interface, the charge of the protein interface [47–50]. In addition, the Coulomb binding free energy [51], ΔG^{coul}_{bind}, which can be computed from $\sum_{i,j} q_i q_j / \varepsilon_{ij} r_{ij}$, where q_i is the charge on atom i, and r_{ij} is the distance between atoms i and j, and the product, Q_1Q_2, of the charges on the components of the complex [26,52,53] have at times been proposed as quantities that correlate highly with SK. However, because the correlations between these empirical quantities and the PBE's predictions of SK are not that strong, their usefulness as predictors of SK is somewhat questionable.

Much interest has been directed at examining the change in SK upon mutation of charged residues [54–56]. These changes can be fairly accurately predicted by the NLPBE [54,57,58], but this method may be more time-consuming than necessary because the terms in the SK predictions of the GB model that contain the interior dielectric constant are small and therefore the exact shape of the molecular interior and the correct choice of dielectric constant should not be particularly important to the PBE's predictions of SK. In addition, the success of the CCT [17,23] combined with several NLPBE studies [22,30] with formal charge distributions indicates that SK is not sensitive to the details of the charge distribution. These findings indicate that the DHE can be used with a formal charge distribution and an approximate structure to rapidly evaluate the rank order of changes in SK upon the mutation of charged residues in protein–nucleic acid complexes. To test this method, we compared its predictions with both experimental binding data for an RNA–protein complex and PBE predictions made by minimizing the structures after mutation and using a realistic charge distribution. The resulting predictions were in close agreement with the available experimental and theoretical data [40–42,54]. Although this method may not prove effective for systems that undergo large conformation changes or pKa shifts upon mutation, it appears that estimating the rank order of changes in SK without additional structural detail or modeling is reasonable for the RNA–protein complexes like those in this study.

2. Methods

2.1. Structure selection and preparation

The nonmutated RNA–protein (peptide) complexes [59–72] in this study were taken from the RCSB Protein Databank [73] and are presented in Table 1. For all of the X-ray structures, all waters and ions were removed, and hydrogens were added with the pdb2pqr [74,75] program. No further energy minimization was performed. For NMR structures, unless otherwise stated, the first model was selected, and the hydrogens in the structure file were used without any further energy minimization. Atomic radii and charge information were taken from the AMBER [76] force field and added to the structure files using the pdb2pqr program. The RNA–protein complex compared to experimental binding data (pdbid: 1JBR) was created in the same manner. In this study, the RNA–peptide data set can be viewed as a subset of the RNA-protein structures.

2.2. Poisson–Boltzmann calculations

Both the linear and nonlinear PBE were solved with a finite difference algorithm developed by Boschitsch and Fenley (submitted to J. Chem. Theory Comput.). The underlying formulation eliminates the self energy terms thus allowing ΔG_{el} to be computed directly without the need for auxiliary electrostatic solvation free energy calculations. The solvent-excluded surface with a probe radius of 1.4 Å was used to define the dielectric boundary of the molecule, and all PBE calculations were performed at 298 K with an exterior dielectric constant of 80 and an interior dielectric constant of 2. The finest grid spacing was set to 0.3 Å, and the 3D grid size was three times the largest dimension of the RNA–protein (peptide) complex. All other PBE parameters were assigned their default values.

ΔG_{el} was computed by taking the difference between the total electrostatic free energy of the complex and the sum of the total electrostatic free energies of the components of the complex in isolation. SK was then computed by taking the slope of the best fit line of the plot of ΔG_{el} versus ln[NaCl] for values of [NaCl]: between 0.1 M and 0.5 M in 0.05 M increments. This is the same procedure used in the experimental measurement of this quantity. As was discussed in Sharp and coworkers [77], $d(\Delta G)/d(\ln[NaCl])$ at any specific salt concentration can also be computed from the osmotic pressure energy contribution to the electrostatic binding free energy. This second estimate is useful for verifying internal consistency and numerically

Table 1
The RCSB Protein Data Bank identification and the corresponding charges and numbers of ion pairs and the charge on the interface with cutoffs of both 4 and 6 Å for the RNA–protein complexes in this study.

PDB Id	RNA charge (e)	Peptide charge (e)	Number of ion pairs		Charge on interface (e)	
			4 Å	6 Å	4 Å	6 Å
1A1T	−19	11	2	5	2	5
1A4T	−14	5	4	5	4	5
1BIV	−27	8	4	7	4	7
1EXY	−32	9	6	7	6	7
1G70	−31	5	2	4	1	3
1HJI	−14	6	2	5	2	5
1I9F	−33	7	4	5	4	4
1MNB	−27	8	3	7	3	7
1NYB	−23	5	4	5	4	5
1QFQ	−14	6	4	5	4	4
1ULL	−34	9	8	10	8	9
1ZBN	−27	9	3	7	3	7
2A9X	−27	7	2	3	2	3
484D	−26	9	7	9	7	9

converged results, and was used to confirm that all results presented here were well converged.

2.3. Computation of the number of ion pairs and the charge at the binding interface

In protein–nucleic acid complexes, the number of ion pairs [44,45] is defined as the number of contacts made between the anionic phosphate groups in the nucleic acid and the cationic amino acid residues (Arg and Lys) in the protein. In the RNA–peptide complexes studied here, the number of ion pairs was determined by calculating the number of Arg and Lys residues within a cutoff distance of any phosphate group in the RNA. If either the NH1 or the NH2 atom of an Arg residue was within the cutoff distance of any OP1 or OP2 atom in the RNA, then this Arg formed one ion pair. Similarly, if the NZ atom of a Lys residue was within the cutoff distance of any OP1 or OP2 atom in the RNA, then this Lys residue formed an ion pair. Each Lys and Arg formed either one or no ion pairs. Two cutoff distances, 4 Å and 6 Å, were used. In this study, potential ion pairs formed by His were ignored, as all His were assumed to be neutral. To calculate the charge on the interface, the OD1 and OD2 atoms of Asp and the OE1 and OE2 atoms of Glu were assumed to form close contacts with the RNA's phosphate groups if they were within the cutoff distance of at least one phosphate group. The number of these close contacts was subtracted from the number of ion pairs to obtain the charge on the binding interface. The resulting numbers of ion pairs and interfacial charges are given in Table 1.

2.4. Preparation and energy minimization protocol for mutant complexes

The mutant RNA–peptide complexes in Supplementary materials Table S1 were constructed from the N-peptide box-B RNA complex (pdbid: 1QFQ) examined previously by García-García and Draper [40], as well as Austin et al. [41,42] The structures for these mutants were created by deleting the appropriate atoms from the native structure from the PDB database and adding any required atoms according to the internal coordinates in the CHARMM force field, followed by a series of energy minimizations using the CHARMM software package [78] as described in Bredenberg and Fenley [51]. The mutated residues in these complexes can be viewed in Supplementary materials.

2.5. Preparation of the mutant RNA-protein complexes for predicting changes in SK with the DHE

The structures of the mutant RNA-protein(peptide) complexes used to predict changes in SK with Eq. (9) were constructed by taking the wild type structure and setting all atoms to zero charge except the NH1 and NH2 atoms of Arg, which were each set to 0.5 e, the OD1 and OD2 atoms of Asp, which were set to −0.5 e, the OE1 and OE2 atoms of Glu, which were set to −0.5 e, the NZ atom of Lys, which was set to 1.0 e, and the OP1 and OP2 atoms of the RNA, which were set to −0.5 e. Charge mutations were then performed by setting any charge on the residue in question to zero.

2.6. Deriving a simplified expression for SK from the generalized Born model

The GB model [35–37] provides a pairwise analytic expression for the electrostatic solvation free energy of a molecule, ΔG_{solv}. If the interior dielectric constant is ϵ_{in} and the exterior dielectric constant is ϵ_{out}, then the GB model predicts that ΔG_{solv} is given by

$$\Delta G_{solv} = -1/2 \sum_{i,j} \frac{q_i q_j}{f_{ij}} \left(\frac{1}{\varepsilon_{in}} - \frac{\exp\left(-\kappa f_{ij}\right)}{\varepsilon_{out}} \right). \quad (1)$$

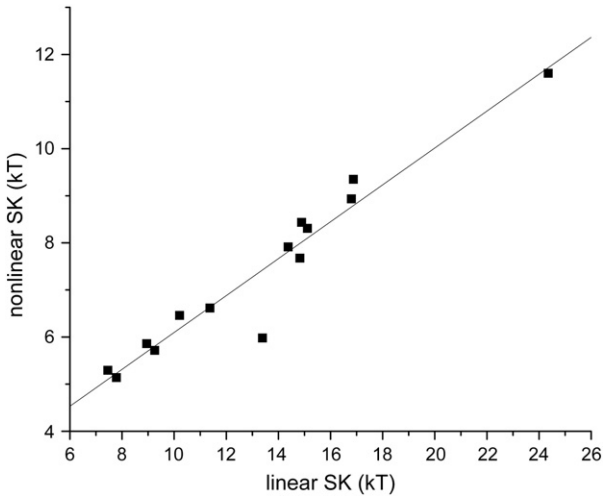

Fig. 1. The derivative, $SK = -\frac{\partial \Delta G_{el}}{\partial \ln[NaCl]}$, of the electrostatic binding free energy, ΔG_{el} with respect to the logarithm of the concentration of 1:1 salt, [NaCl], in units of kT predicted by the nonlinear Poisson–Boltzmann equation, PBE, plotted against the predictions of the linear PBE for the RNA–peptide complexes in this study. The slope of the best-fit line is 0.4, and $R^2 = 0.94$.

In this equation, q_i is the charge on the i'th atom, and κ is the Debye–Hückel screening parameter, given by

$$\kappa = \left(\frac{8\pi N_A e^2 I}{1000 k_B T \varepsilon_{out}} \right)^{1/2} \quad (2)$$

where N_A is Avogadro's number, I is the ionic strength of the solution, k_B is Boltzmann's constant, and T is the absolute temperature. The f_{ij} in Eq. (1) are computed from

$$f_{ij} = \left(r_{ij}^2 + B_i B_j \exp\left(-r_{ij}^2 / 4 B_i B_j \right) \right)^{1/2} \quad (3)$$

where r_{ij} is the distance between atoms i and j. B_i is the Born radius, which can be calculated from

$$\Delta G_{solv}^{i} = -\frac{q_i^2}{2B_i} (1/\varepsilon_{in} - 1/\varepsilon_{out}) \quad (4)$$

where ΔG_{solv}^{i} is the polar solvation free energy of a molecule with the same distribution of interior and exterior dielectric constants as the original molecule at zero salt concentration, but with all charges except q_i set to zero. The form of f_{ij} is selected to interpolate between the analytical solution to the PBE for two widely separated spheres, which is given by the DHE, and the analytical solution for a single sphere. In practice, these Born radii are calculated by an analytical approximation.

By using the free energy cycle in Fig. 2, ΔG_{el} can be computed by

$$\Delta G_{el} = \Delta G_{bind}^{coul} + \Delta G_{solv}^{comp} - \left(\Delta G_{solv}^{1} + \Delta G_{solv}^{2} \right) \quad (5)$$

where ΔG_{bind}^{coul} is the Coulomb binding free energy given by

$$\Delta G_{bind}^{coul} = 1/2 \sum_{\substack{i,j \\ \text{inter}}} \frac{q_i q_j}{\varepsilon_{in} r_{ij}} \quad (6)$$

where the summation is taken over all those pairs of atoms which have one member in each component of the complex. Because the dielectric environment of each atom changes upon binding, B_i is different in the bound and unbound states, and therefore f_{ij} is different in the bound and unbound states as well. By combining Eqs. (1), (5),

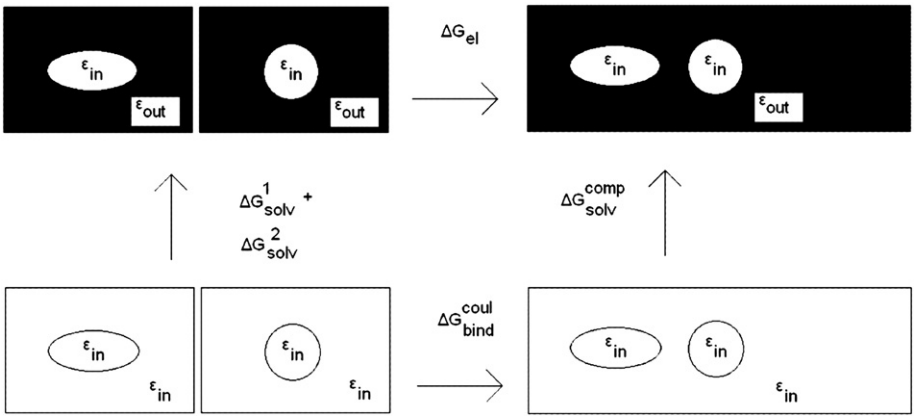

Fig. 2. The free energy cycle used to compute the electrostatic binding free energy, ΔG_{el} in Eq. (5). ΔG_{el}^{coul} is the Coulombic binding free energy, ΔG_{solv}^{i} is the electrostatic solvation free energy of component i of the complex, and ΔG_{solv}^{comp} is the electrostatic solvation free energy of the complex.

and (6), defining f_{ij}^{comp} to be f_{ij} for the i–j'th atom pair in the complex, f_{ij}^{k} to be f_{ij} for the i–j'th atom pair in the k'th component of the complex, and defining inter to designate summations over all atom pairs with one atom in each component of the complex, ΔG_{el} can be written as

$$\begin{aligned}\Delta G_{el} = {} & -1/2\sum_{\substack{i,j\\ \text{inter}}}\frac{q_iq_j}{\varepsilon_{in}}\left(\frac{1}{f_{ij}^{comp}}-\frac{1}{r_{ij}}\right)-1/2\sum_{\substack{i,j\\ 1}}\frac{q_iq_j}{\varepsilon_{in}}\left(\frac{1}{f_{ij}^{comp}}-\frac{1}{f_{ij}^{1}}\right)\\ & -1/2\sum_{\substack{i,j\\ 2}}\frac{q_iq_j}{\varepsilon_{in}}\left(\frac{1}{f_{ij}^{comp}}-\frac{1}{f_{ij}^{2}}\right)-1/2\sum_{\substack{i,j\\ 1}}\frac{q_iq_j}{\varepsilon_{out}}\left(\frac{\exp\left(-\kappa f_{ij}^{comp}\right)}{f_{ij}^{comp}}-\frac{\exp\left(-\kappa f_{ij}^{1}\right)}{f_{ij}^{1}}\right)\\ & -1/2\sum_{\substack{i,j\\ 2}}\frac{q_iq_j}{\varepsilon_{out}}\left(\frac{\exp\left(-\kappa f_{ij}^{comp}\right)}{f_{ij}^{comp}}-\frac{\exp\left(-\kappa f_{ij}^{2}\right)}{f_{ij}^{2}}\right)\\ & -1/2\sum_{\substack{i,j\\ \text{inter}}}\frac{q_iq_j}{\varepsilon_{out}}\frac{\exp\left(-\kappa f_{ij}^{comp}\right)}{f_{ij}^{comp}}\end{aligned} \tag{7}$$

where the second and fourth summations are taken over the first component of the complex and the third and fifth summations are taken over the second component of the complex. The GB's predictions of SK can be derived from this equation by taking the derivative of ΔG_{el} with respect to ln[NaCl]:

$$\begin{aligned}SK = -\frac{\partial\Delta G_{el}}{\partial \ln[\mathrm{NaCl}]} &= -\kappa/2\frac{\partial\Delta G_{el}}{\partial\kappa}\\ &= -\kappa/4\sum_{\substack{i,j\\ 1}}\frac{q_iq_j}{\varepsilon_{out}}\left(\exp\left(-\kappa f_{ij}^{comp}\right)-\exp\left(-\kappa f_{ij}^{1}\right)\right)\\ &\quad -\kappa/4\sum_{\substack{i,j\\ 2}}\frac{q_iq_j}{\varepsilon_{out}}\left(\exp\left(-\kappa f_{ij}^{comp}\right)-\exp\left(-\kappa f_{ij}^{2}\right)\right)\\ &\quad -\kappa/4\sum_{\substack{i,j\\ \text{inter}}}\frac{q_iq_j}{\varepsilon_{out}}\exp\left(-\kappa f_{ij}^{comp}\right).\end{aligned} \tag{8}$$

If $f_{ij}^{comp}\approx f_{ij}^{k}$ for atom pairs with both atoms in the same component of the complex, then the first two summations in this equation will be much smaller than the third, and they can thus be neglected. If the further assumption that $f_{ij}^{comp}\approx r_{ij}$ for atom pairs with one atom in each component of the complex, then Eq. (8) reduces to the DHE's [38] prediction of SK:

$$SK\approx -\kappa/4\sum_{\substack{i,j\\ \text{inter}}}\frac{q_iq_j}{\varepsilon_{out}}\exp\left(-\kappa r_{ij}\right). \tag{9}$$

The validity of the approximations leading from Eq. (8) to Eq. (9) is demonstrated in Table S2 of the Supplementary materials.

3. Results

3.1. Comparing the nonlinear PBE's predictions of SK to those of the linear PBE

As mentioned above, the NLPBE is taken as the gold standard of comparison in this study because it has been used successfully to predict SK for many biomolecular complexes, but the impossibility of analytically solving the NLPBE for a general geometry makes determining which physical properties determine SK difficult. Instead, the linear PBE and the derived GB model permit the formulation of an analytical expression for SK which can be used to determine which physical properties determine SK. It has been noted, however, in several studies and is clear from Fig. 1 that the linear PBE overestimates the magnitude of SK [30,33,57], and the ratio between the linear PBE's predictions of SK and those of the NLPBE appears to grow with increasing charge on the biomolecular complex. Fortunately however, this ratio appears to grow relatively slowly with charge because SK computed with the NLPBE is proportional to SK computed with the linear PBE for the RNA–peptide complexes considered here, as can be seen from Fig. 1. The slope of this line is 0.4 with a correlation factor $R^2 = 0.94$. Therefore, it appears that the linear PBE remains useful for computing the rank order of the change in SK for different charge mutations if the charge of the complex is kept fairly constant.

3.2. Generalized Born analysis

Eq. (9) approximates the PBE, and its predictions will fail in any situation where the PBE itself will fail. In addition, the method presented in this paper assumes that the bound conformation of the molecule is identical to the unbound state, and thus if the protein undergoes either extensive conformational changes or pKa shifts upon binding then this expression will fail. Extending this method to account for these effects may be possible by taking multiple snapshots

from molecular mechanics trajectories, but because the amount of conformational flexibility can vary significantly from complex to complex, the errors will be highly system dependent. In addition, the PBE itself is only really valid for either 1:1 salt or mixed salt conditions with small quantities 2:1 salt because the PBE occasionally fails to predict either the correct distribution of ions or the correct salt dependence of the folding free energy for nucleic acid systems with multivalent ions because of its lack of ion–ion correlations [79–86]. The present method could perhaps be improved by using a theory that includes such effects, but for small concentrations of $MgCl_2$ and for molecules with comparable or lower charge densities than those used here, the results are probably reasonable [55,87,88].

To test Eq. (9), we examined a series of RNA–binding peptide complexes with an arginine-rich (ARM) binding motif. A typical example of such a complex (pdbid: 1QFQ) is shown in Fig. S1 of the Supplementary materials. As is typical of nucleic acid-binding proteins, a large number of positively charged residues, Lys and Arg, form close contacts with the phosphate groups of the nucleic acid, but the proteins considered in this study can contain both a significant number of anionic residues and more distant cationic residues. Although these have traditionally been considered as unimportant to SK because they are typically fairly distant from the binding interface, Eq. (9) indicates that they should contribute to SK, and this finding agrees with those of earlier studies [33,40], where both distant and anionic residues contributed significantly to SK. In Fig. 3, the PBE's predictions of SK for the complexes in Table 1 are plotted against the predictions of Eq. (9). This line has a correlation of $R^2 = 0.95$. Unfortunately, the slope of the line is not 1, but rather 0.57. As described above, the slope of this line reflects the difference between the linear and nonlinear PBE's predictions of SK. However, apparently the nonlinearity does not change much over the charges considered in this study, allowing Eq. (9) to predict correctly the rank order of SK even if the absolute difference in SK between different complexes is overestimated.

One consequence of Eq. (9) that is superficially troubling is that it predicts that SK is not constant with respect to salt concentration. In fact, for some of the complexes in Table 1, Eq. (9) predicts that SK at a salt concentration of 0.5 M is 1/2 of that at a salt concentration of 0.1 M. This would seem to contradict the findings of experimental studies that SK is constant over a range of salt concentrations. However, this discrepancy can be partially explained by Fig. 4, which plots ΔG_{el} predicted by the PBE as a function of ln[NaCl] for a typical example of the complexes (PDB id 2A9X) in this study and Fig. 5, which plots the change in osmotic pressure upon binding as a function of ln[NaCl], which, as shown by Sharp and coworkers [77], equals the derivative of ΔG_{el} with respect to ln[NaCl]. Although Fig. 4 appears to be roughly linear, with a best fit line with an $R^2 = 0.99$, its derivative changes by a significant amount between 0.1 and 0.4 M, as shown in Fig. 5. The problem of a nonconstant SK can be overcome by selecting a salt concentration of 0.25 M for computing SK with Eq. (9), as then the predictions of the DHE agree with those PBE's predictions of SK as illustrated in Fig. 3.

3.3. Explaining why the PBE's predictions of ΔGel differ from those of the DHE

Much of the interest in SK has been driven by a desire to use experimental data on SK in conjunction with the total binding free energy to obtain estimates of ΔG_{el} and its nonelectrostatic counterpart, both of which cannot be obtained directly from experimental binding data. Unfortunately, the predictions of ΔG_{el} by the PBE do not support the assumed proportionality between SK and ΔG_{el} upon which this common experimental practice is based. The lack of correlation between these two quantities arises because the approximations that lead from Eq. (8) to Eq. (9) cannot be applied to Eq. (7) to simplify the predictions of ΔG_{el} by the PBE to those of the DHE.

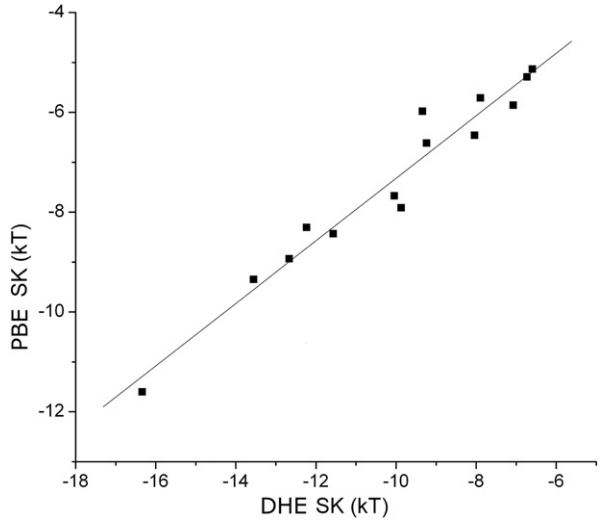

Fig. 3. SK in units of kT predicted by the nonlinear Poisson–Boltzmann equation, NLPBE, for the biomolecular complexes listed in Table 1 versus the predictions of SK given by the Debye–Hückel equation at a salt concentration of 0.25 M, which are also the simplified predictions of the generalized Born, GB, model, given in Eq. (9). The slope of the best-fit line is 0.57, and $R^2 = 0.95$.

Instead, the first three summations in Eq. (7), which disappear when the derivative with respect to salt concentration is taken, are divided by ε_{in} rather than ε_{out}. These terms are therefore comparable in magnitude to the final DHE-like term in Eq. (7), and the PBE's predictions of ΔG_{el} therefore differ from those of the DHE. The lack of proportionality between SK and ΔG_{el} is clear from Fig. 6 where the PBE's predictions of ΔG_{el} for the RNA–peptide complexes in Table 1 are plotted against its predictions of SK, and this conclusion is relatively independent of the exact treatment of the molecular boundary, as long as the molecular interior is assumed to have a substantially smaller dielectric constant than the solvent, in agreement with our findings for small cationic drugs binding DNA[30].

3.4. Relating empirical quantities to SK

As discussed in the introduction, many quantities have been observed to be correlated with SK, including the number of ion pairs, the charge of the ligand's binding interface, ΔG^{coul}_{bind}, and Q_1Q_2. All of

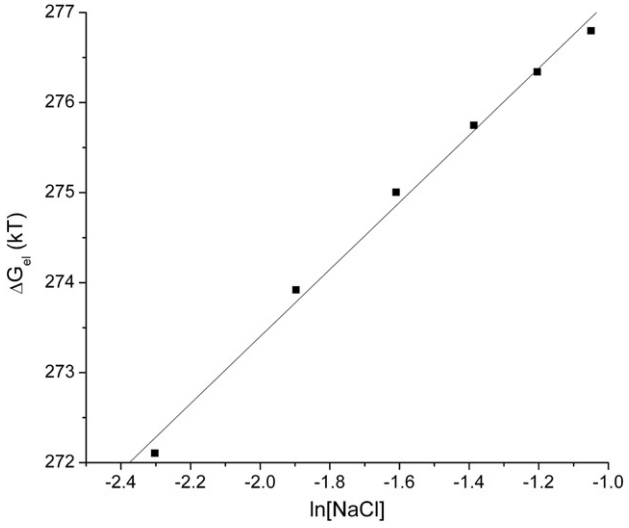

Fig. 4. ΔG_{el} in units of kT computed with the NLPBE plotted against the logarithm of the salt concentration, ln[NaCl], for a typical RNA–peptide complex in this study (PDB id 2a9x). The points are roughly linear, with $R^2 = 0.99$.

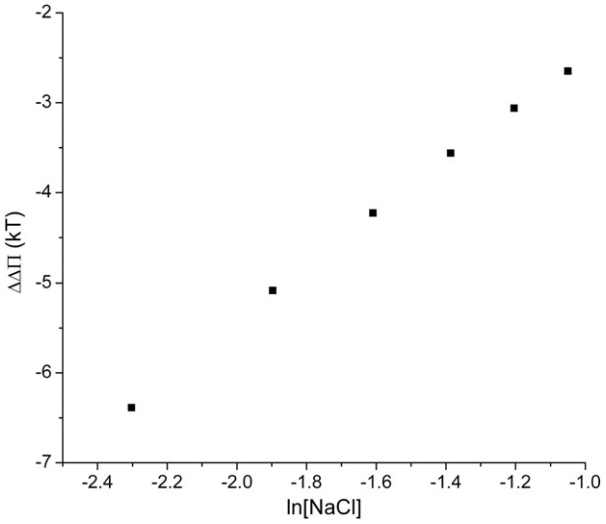

Fig. 5. The change in osmotic pressure upon binding for the RNA–peptide complex in Fig. 5 (PDB id 2a9x) computed with the NLPBE in units of kT plotted against the logarithm of the salt concentration, ln[NaCl].

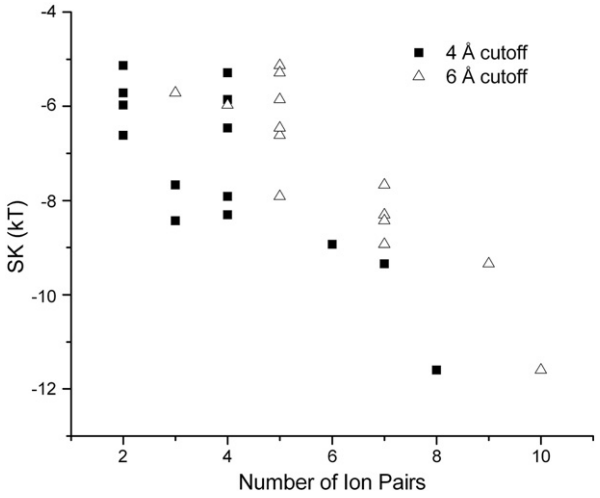

Fig. 7. SK in units of kT computed with the NLPBE for the RNA–peptide complexes in Table 1 plotted against the number of ion pairs with cutoffs of both 4 and 6 Å. $R^2 = 0.65$ and 0.81, respectively.

these quantities can be viewed as approximations to Eq. (9) made by replacing the exponential decay in the contribution of each atom pair to SK with a simpler function. Using the number of ion pairs or the charge of the ligand's binding interface is equivalent to replacing the exponential decay with a step function, using ΔG_{bind}^{coul} is equivalent to replacing the exponential decay with a $1/r$ decay, and using Q_1Q_2 is equivalent to replacing the exponential decay with a constant. However, because Eq. (9) can be derived from the GB or DHE with fewer intermediate approximations, it should be a better predictor of SK than any of these empirical quantities.

In Fig. 7, SK computed with the PBE is plotted against the number of ion pairs with cutoff distances of both 4 and 6 Å. The resulting correlations are significantly weaker than that in Fig. 3, with R^2 values of 0.65 and 0.81, respectively. In addition, using the number of ion pairs to estimate SK ignores the effects of both distant and anionic residues which, as shown in earlier studies, is not valid [33,40]. The deviation between the number of ion pairs and SK would therefore be expected to increase for larger molecules with more distant charged residues, indicating that the usefulness of the common assumption [16,54] that SK is proportional to the number of ion pairs is questionable.

As can be seen in Table 1, the interfacial charge of the peptide was almost the same as the number of ion pairs at either cutoff distance. This observation reflects the lack of anionic residues in the binding interface of the peptides used in this study. Surprisingly, the correlation between the interfacial charge and SK is worse than that between the number of ion pairs and SK, as with a cutoff distance of 4 Å, R^2 falls to 0.63 and with a 6 Å cutoff it falls to 0.71. At any rate, using the interfacial charge to predict SK faces the same challenges as using the number of ion pairs, and so the usefulness of this proposed correlation is questionable.

In Fig. 8, SK computed with the PBE is plotted against ΔG_{bind}^{coul}. With an $R^2 = 0.89$, this correlation is weaker than that in Fig. 3, and because of the lack of the exponential decay in Eq. (9), this correlation would be expected to be even worse for larger, more complex biomolecules. Eq. (9) therefore appears to be a superior predictor of SK.

In Fig. 9, SK computed with the PBE is plotted against Q_1Q_2. This quantity would be expected to be an accurate predictor of SK as the salt concentration declines to zero,[52] but for the moderate salt concentrations used in this study, the correlation, with an $R^2 = 0.73$, is not very useful. Once again, Eq. (9) appears to be a more useful method to predict SK.

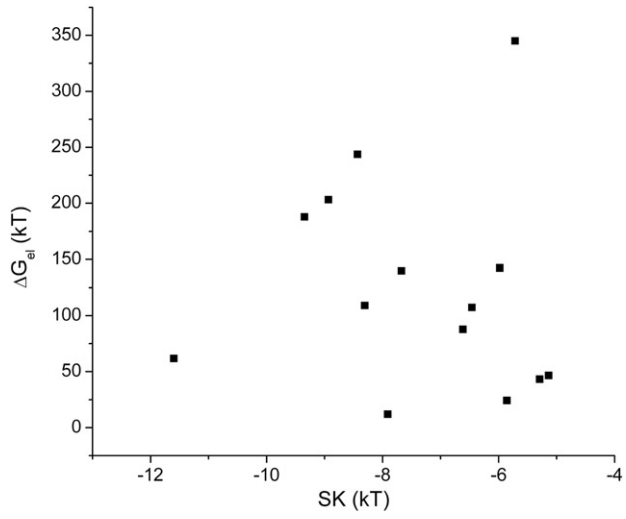

Fig. 6. ΔG_{el} in units of kT calculated with the NLPBE plotted against SK in units of kT for the RNA–peptide complexes in Table 1. These two quantities are not correlated.

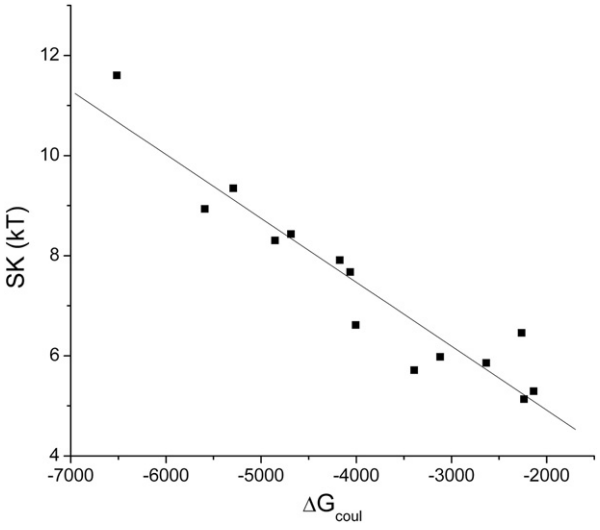

Fig. 8. SK in units of kT computed with the NLPBE for the RNA-protein complexes in Table 1 plotted against the Coulomb binding free energy, ΔG_{bind}^{coul}. $R^2 = 0.89$.

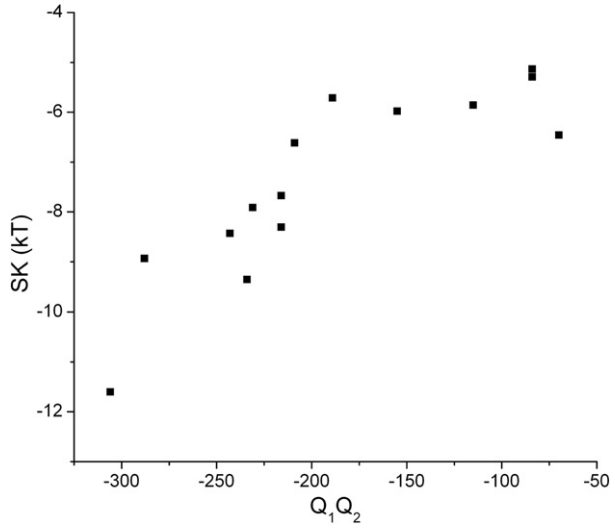

Fig. 9. SK in units of kT computed with the PBE for the RNA–protein complexes in Table 1 plotted against the product, Q_1Q_2, of the charges on the components of the complex. $R^2 = 0.73$.

3.5. Quickly predicting the rank order of changes in SK upon mutation of charged residues in RNA–peptide complexes

Because the terms that depend on the definition of the molecular interior (those that include f_{ij}) disappear while deriving Eq. (9) from the GB model, SK does not appear to depend strongly on the precise form of the molecular surface dividing space into interior and exterior dielectric regions. In addition, because of the correlations with the number of ion pairs and Q_1Q_2, SK does not appear to strongly depend on the exact charge distribution. In conclusion, considering these two facts, we propose a simple approach of predicting the change in SK upon the mutation of charged residues: use a formal charge distribution, as described in the methods, Eq. (9), and the native structure of the complex in combination with simply adding or removing charges to reflect charge mutations.

To test this proposed method, we plotted in Fig. 10 SK predicted by this simple method against SK predicted by the more rigorous method nonlinear PBE method described in Methods, for all of the mutant complexes of the N-peptide box-B system listed in Supplementary materials Table S1. The predictions are highly correlated, with an $R^2 = 0.90$ and a slope of $m = 0.87$. Although this correlation is weaker than that noted in Fig. 3, it is still strong considering that no account was taken of possible changes in the molecular surface upon mutation and that a formal charge distribution was used. The slope of this line is not 1, but the rank order of SK for these complexes is preserved, and given the high correlation of these results, this method appears to reproduce well the predictions of the NLPBE.

This method also appears capable of reproducing the results of experimental binding measurements, as can be seen from Fig. 11, where the experimentally-determined SK for several mutants of the RNA–protein complex (pdbid: 1JBR) studied by Plantinga et al. [54] is plotted against the predictions of the DHE with a formal charge distribution. The residues that were mutated and the tabulated data can be seen in the Supplementary materials. The two sets of predictions in Fig. 11 are highly correlated, with a best-fit line with an $R^2 = 0.84$, which is only slightly worse than the agreement with the PBE given in the original study. This correlation could possibly be improved by taking into account the proper protonation state of the His residue mutated in one of the complexes. In addition, the rank order of changes in SK was well predicted by the GBSK, as was true in the NLPBE, as noted by Plantinga et al. [54].

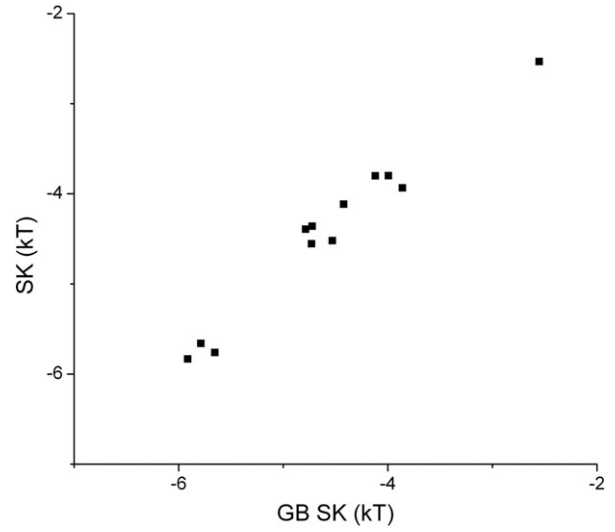

Fig. 10. SK in units of kT computed with the NLPBE of mutants of the λN peptide-box B hairpin RNA complex (pdb id: 1QFQ) whose structures were created with the detailed structure preparations described in the Methods plotted against SK in units of kT computed with Eq. (9) (GBSK) at [NaCl] = 0.25 M with structures that were created with formal charges, the DHE, and the native structure, as outlined in the Methods. The slope of the best-fit line is 0.87, and $R^2 = 0.90$.

4. Conclusions

Earlier studies have demonstrated that SK predicted by the PBE agrees well with both experimental data and the CCT [89]. However, as shown in the results and in agreement with an earlier study [30], on DNA-binding drugs, the CCT's predictions of ΔG_{el} do not agree with those of the PBE with a dielectric discontinuity, but explaining the discrepancy between the two theories is difficult because the PBE is not analytical. Understanding this discrepancy is important because the lack of proportionality between these two quantities calls into question the commonly-used method of parsing the experimental binding free energy into electrostatic and nonelectrostatic components by assuming the validity of this relationship [31].

The derivation leading to Eq. (9) illustrates that the PBE's predictions of SK can be simplified to those of the DHE, but, a similar simplification of Eq. (7) is impossible because the first three summations are comparable in magnitude to the final DHE-like

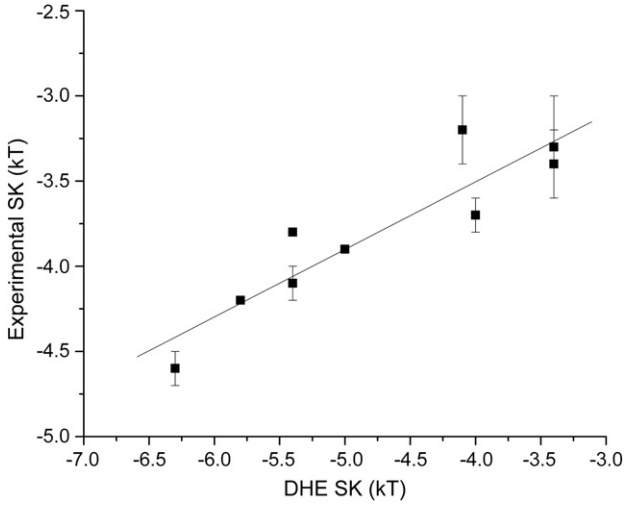

Fig. 11. The experimentally-determined SK for the mutants of the ribotoxin restrictocin–RNA complex (pdbid: 1JBR) complex examined by Plantinga et al. [54] plotted against SK in units of kT computed with Eq. (9) (DHESK) at [NaCl] = 0.25 M with structures that were created with formal charges, the DHE, and the native structure, as outlined in the Methods. The slope of the best-fit line is 0.3, and $R^2 = 0.84$.

term. This impossibility explains the lack of correlation between ΔG_{el} and SK in the presence of a dielectric discontinuity mentioned above. In addition, Eq. (9) explains the observed correlations between SK and quantities like the number of ion pairs, the charge at the interface, ΔG_{bind}^{coul}, and Q_1Q_2. Because the predictions of SK by these quantities are inferior to those of Eq. (9), their usefulness is somewhat questionable.

SK does not appear to be highly sensitive to either small changes in the definition of the molecular surface or different charge distributions. This leads to the idea that predicting the rank order of changes in SK caused by the mutation of charged residues with simply a formal charge distribution, the complex's native structure, and Eq. (9) could be possible. As shown above, this simple method agrees well with the predictions of more rigorous PBE calculations using mutant structures predicted by molecular mechanics calculations as well as the results of experimental thermodynamic binding studies.

Supplementary materials related to this article can be found online at doi:10.1016/j.bpc.2011.02.010.

Acknowledgments

One of the authors (MOF) acknowledges the support from NIH-GM078538-01 (PI: Dr. Michael S. Chapman, OHSU, Co-PI: MOF). Both authors MOF and AHB acknowledge support from SBIR NIH 2R446M073391-02.

References

[1] D.P. Mascotti, T.M. Lohman, Thermodynamics of single-stranded RNA binding to oligolysines containing tryptophan, Biochemistry 31 (1992) 8932–8946.
[2] D.P. Mascotti, T.M. Lohman, Thermodynamics of single-stranded RNA and DNA interactions with oligolysines containing tryptophan. Effects of base composition, Biochemistry 32 (1993) 10568–10579.
[3] D.P. Mascotti, T.M. Lohman, Thermodynamics of Oligoarginines binding to RNA and DNA, Biochemistry 36 (1997) 7272–7279.
[4] B.A. Todd, D.C. Rau, Interplay of ion binding and attraction in DNA condensed by multivalent cations, Nucleic Acids Res. 36 (2008) 501–510.
[5] M.M. Islam, P. Pandya, S. Kumar, G.S. Kumar, RNA targeting through binding of small molecules: studies on t-RNA binding by the cytotoxic protoberberine alkaloid coralyne, Mol. Biosyst. 5 (2009) 244–254.
[6] M.M. Islam, S.R. Chowdhury, G.S. Kumar, Spectroscopic and calorimetric studies on the binding of alkaloids berberine, palmatine and coralyne to double stranded RNA polynucleotides, J. Phys. Chem. B 113 (2009) 1210–1224.
[7] M. Kaul, D.S. Pilch, Thermodynamics of aminoglycoside—rRNA recognition: the binding of neomycin-class aminoglycosides to the A site of 16S rRNA, Biochemistry 41 (2002) 7695–7706.
[8] A. Paleskava, A.L. Konevega, M.V. Rodnina, Thermodynamic and kinetic framework of selenocysteyl-tRNASec recognition by elongation factor SelB, J. Biol. Chem. 285 (2010) 3014–3020.
[9] S.G. Williams, K.B. Hall, Coevolution of Drosophila snf protein and its snRNA targets, Biochemistry 49 (2010) 4571–4582.
[10] N. Korolev, N.V. Berezhnoy, K.D. Eom, J.P. Tam, L. Nordenskiold, A universal description for the experimental behavior of salt-(in)dependent oligocation-induced DNA condensation, Nucleic Acids Res. 37 (2009) 7137–7150.
[11] T.C. Weiss, G.G. Zhai, S.S. Bhatia, P.J. Romaniuk, An RNA aptamer with high affinity and broad specificity for zinc finger proteins, Biochemistry 49 (2010) 2732–2740.
[12] S.S. Athavale, W. Ouyang, M.P. McPike, B.S. Hudson, P.N. Borer, Effects of the nature and concentration of salt on the interaction of the HIV-1 nucleocapsid protein with SL3 RNA, Biochemistry 49 (2010) 3525–3533.
[13] H. Xi, S. Kumar, L. Dosen-Micovic, D.P. Arya, Calorimetric and spectroscopic studies of aminoglycoside binding to AT-rich DNA triple helices, Biochimie (2010) 514–529.
[14] P.C. Bevilacqua, T.R. Cech, Minor-groove recognition of double-stranded RNA by the double-stranded RNA-binding domain from the RNA-activated protein kinase PKR, Biochemistry 35 (1996) 9983–9994.
[15] H. Suryawanshi, H. Sabharwal, S. Maiti, Thermodynamics of peptide—RNA recognition: the binding of a Tat peptide to TAR RNA, J. Phys. Chem. B 114 (2010) 11155–11163.
[16] S.H. Mishra, A.M. Spring, M.W. Germann, Thermodynamic profiling of HIV RREIIB RNA-zinc finger interactions, J. Mol. Biol. 393 (2009) 369–382.
[17] M.T. Record Jr., W. Zhang, C.F. Anderson, Analysis of effects of salts and uncharged solutes on protein and nucleic acid equilibria and processes: a practical guide to recognizing and interpreting polyelectrolyte effects, Hofmeister effects, and osmotic effects of salts, Adv. Protein Chem. 51 (1998) 281–353.
[18] V.K. Misra, K.A. Sharp, R.A. Friedman, B. Honig, Salt effects on ligand-DNA binding: minor groove binding antibiotics, J. Mol. Biol. 238 (1994) 245–263.
[19] V.K. Misra, J.L. Hecht, K.A. Sharp, R.A. Friedman, B. Honig, Salt effects on protein–DNA interactions: the λ cI repressor and EcoRI endonuclease, J. Mol. Biol. 238 (1994) 264–280.
[20] M. Zacharias, B.A. Luty, M.E. Davis, J.A. McCammon, Poisson–Boltzmann analysis of the λ repressor–operator interaction, Biophys. J. 63 (1992) 1280–1285.
[21] V.K. Misra, B. Honig, On the magnitude of the electrostatic contribution to ligand–DNA interactions, Proc. Natl Acad. Sci. U.S.A. 92 (1995) 4691–4695.
[22] J.M. Blose, D.J. Proctor, N. Veeraraghavan, V.K. Misra, P.C. Bevilacqua, Contribution of the closing base pair to exceptional stability in RNA tetraloops: roles for molecular mimicry and electrostatic factors, J. Am. Chem. Soc. 131 (2009) 8474–8484.
[23] G.S. Manning, The molecular theory of polyelectrolyte solutions with applications to the electrostatic properties of polynucleotides, Q. Rev. Biophys. 11 (1978) 179–246.
[24] I. Rouzina, V.A. Bloomfield, Macroion attraction due to electrostatic correlation between screening counterions. 1. Mobile surface-adsorbed ions and diffuse ion cloud, J. Phys. Chem. 100 (1996) 9977–9989.
[25] I. Rouzina, V.A. Bloomfield, Competitive electrostatic binding of charged ligands to polyelectrolytes: planar and cylindrical geometries, J. Phys. Chem. 100 (1996) 4292–4304.
[26] A.V. Sivolob, S.N. Khrapunov, Binding of positively charged ligands to DNA. Effects of ionic strength, ligand charge and size, Mol. Biol. 22 (1988) 414–422.
[27] D. Stigter, K.A. Dill, Binding of ionic ligands to polyelectrolytes, Biophys. J. 71 (1996) 2064–2074.
[28] B.Z. Lu, Y.C. Zhou, M.J. Holst, J.A. McCammon, Recent progress in numerical methods for the Poisson–Boltzmann Equation in biophysical applications, Commun Comput Phys. 3 (2008) 973–1009.
[29] A.H. Boschitsch, M.O. Fenley, Hybrid boundary element and finite difference method for solving the nonlinear Poisson–Boltzmann equation, J. Comput. Chem. 25 (2004) 935–955.
[30] M.O. Fenley, R.C. Harris, B. Jayaram, A.H. Boschitsch, Revisiting the association of cationic groove-binding drugs to DNA using a Poisson–Boltzmann approach, Biophys. J. (2010) 879–886.
[31] M.T. Record Jr., T.M. Lohman, P.L. deHaseth, Ion effects on ligand-nucleic acid interactions, J. Mol. Biol. 107 (1976) 145–158.
[32] T. Murtola, I. Vattulainen, E. Falck, Insights into activation and RNA binding of trp RNA-binding attenuation protein (TRAP) through all-atom simulations, Proteins 71 (2008) 1995–2011.
[33] J.H. Bredenberg, A.H. Boschitsch, M.O. Fenley, The role of anionic protein residues on the salt dependence of the binding of aminoacyl-tRNA: synthetases to tRNA: a Poisson–Boltzmann analysis, Commun. Comput. Phys. 3 (2008) 1051–1070.
[34] J. Eargle, A.A. Black, A. Sethi, L.G. Trabuco, Z. Luthey-Schulten, Dynamics of recognition between tRNA and elongation factor Tu, J. Mol. Biol. 377 (2008) 1382–1405.
[35] W.C. Still, A. Tempczyk, R.C. Hawley, T. Hendrickson, Semianalytical treatment of solvation for molecular mechanics and dynamics, J. Am. Chem. Soc. 112 (1990) 6127–6129.
[36] D. Bashford, D.A. Case, Generalized born models of macromolecular solvation effects, Annu. Rev. Phys. Chem. 51 (2000) 129–152.
[37] J. Srinivasan, M.W. Trevathan, P. Beroza, D.A. Case, Application of a pairwise generalized Born model to proteins and nucleic acids: inclusion of salt effects, Theor. Chem. Acc. 101 (1999) 426–434.
[38] R.A. Robinson, R.H. Stokes, Electrolyte Solutions, Courier Dover Publications, 2002.
[39] D. Matulis, I. Rouzina, V.A. Bloomfield, Thermodynamics of DNA binding and condensation: isothermal titration calorimetry and electrostatic mechanism, J. Mol. Biol. 296 (2000) 1053–1063.
[40] C. García-García, D.E. Draper, Electrostatic interactions in a peptide-RNA complex, J. Mol. Biol. 331 (2003) 75–88.
[41] R.J. Austin, T. Xia, J. Ren, T.T. Takahashi, R.W. Roberts, Designed arginine-rich RNA-binding peptides with picomolar affinity, J. Am. Chem. Soc. 124 (2002) 10966–10967.
[42] R.J. Austin, T. Xia, J. Ren, T.T. Takahashi, R.W. Roberts, Differential modes of recognition in N peptide—BoxB complexes, Biochemistry 42 (2003) 14957–14967.
[43] X. Qi, T. Xia, R.W. Roberts, Acridine—N peptide conjugates display enhanced affinity and specificity for boxB RNA targets, Biochemistry 49 (2010) 5782–5789.
[44] L. Jen-Jacobson, M. Kurpiewski, D. Lesser, J. Grable, H.W. Boyer, J.M. Rosenberg, P.J. Greene, Coordinate ion pair formation between EcoRI endonuclease and DNA, J. Biol. Chem. 258 (1983) 14638–14646.
[45] D.J. Barlow, J.M. Thornton, Ion-pairs in proteins, J. Mol. Biol. 168 (1983) 867–885.
[46] J.K. Abrahamson, T.M. Laue, D.L. Miller, A.E. Johnson, Direct determination of the association constant between elongation factor Tu. GTP and aminoacyl-tRNA using fluorescence, Biochemistry 24 (1985) 692–700.
[47] I.A. Shkel, J.D. Ballin, M.T. Record Jr., Interactions of cationic ligands and proteins with small nucleic acids: analytic treatment of the large Coulombic end effect on binding free energy as a function of salt concentration, Biochemistry 45 (2006) 8411–8426.
[48] R.M. Saecker, M.T. Record Jr., Protein surface salt bridges and paths for DNA wrapping, Curr. Opin. Struct. Biol. 12 (2002) 311–319.
[49] W.S. Kontur, M.W. Capp, T.J. Gries, R.M. Saecker, M.T. Record Jr., Probing DNA binding, DNA opening, and assembly of a downstream clamp/jaw in *Escherichia coli* RNA polymerase-lambdaP(R) promoter complexes using salt and the physiological anion glutamate, Biochemistry 49 (2010) 4361–4373.
[50] K.A. Vander Meulen, R.M. Saecker, M.T. Record Jr., Formation of a wrapped DNA-protein interface: experimental characterization and analysis of the large contributions of ions and water to the thermodynamics of binding IHF to H'DNA, J. Mol. Biol. 377 (2008) 9–27.
[51] J.H. Bredenberg, M.O. Fenley, Salt dependent association of novel mutants of TATA-binding proteins to DNA: predictions from theory and experiments, Commun. Comput. Phys. 3 (2008) 1132–1153.

[52] A.H. Boschitsch, M.O. Fenley, H.X. Zhou, Fast boundary element method for the linear Poisson–Boltzmann equation, J. Phys. Chem. 106 (2002) 2741–2754.
[53] K. Talley, P. Kundrotas, E. Alexov, Modeling salt dependence of protein–protein association: linear vs non-linear Poisson–Boltzmann equation, Commun. Comput. Phys. 3 (2008) 1071–1086.
[54] M.J. Plantinga, A.V. Korennykh, J.A. Piccirilli, C.C. Correll, Electrostatic interactions guide the active site face of a structure-specific ribonuclease to its RNA substrate, Biochemistry 47 (2008) 8912–8918.
[55] D. GuhaThakurta, D.E. Draper, Contributions of basic residues to ribosomal protein L11 recognition of RNA, J. Mol. Biol. 295 (2000) 569–580.
[56] M.J. Law, M.E. Linde, E.J. Chambers, C. Oubridge, P.S. Katsamba, L. Nilsson, I.S. Haworth, I.A. Laird-Offringa, The role of positively charged amino acids and electrostatic interactions in the complex of U1A protein and U1 hairpin II RNA, Nucleic Acids Res. 34 (2006) 275–285.
[57] J.H. Bredenberg, C. Russo, M.O. Fenley, Salt-mediated electrostatics in the association of TATA binding proteins to DNA: a combined molecular mechanics/Poisson–Boltzmann study, Biophys. J. 94 (2008) 4634–4645.
[58] R.P. Bahadur, S. Kannan, M. Zacharias, Binding of the bacteriophage P22 N-peptide to the boxB RNA motif studied by molecular dynamics simulations, Biophys. J. 97 (2009) 3139–3149.
[59] R.N. De Guzman, Z.R. Wu, C.C. Stalling, L. Pappalardo, P.N. Borer, M.F. Summers, Structure of the HIV-1 nucleocapsid protein bound to the SL3 Ψ-RNA recognition element, Science 279 (1998) 384–388.
[60] Z. Cai, A. Gorin, R. Frederick, X. Ye, W. Hu, A. Majumdar, A. Kettani, D.J. Patel, Solution structure of P22 transcriptional antitermination N peptide–box B RNA complex, Nat. Struct. Mol. Biol. 5 (1998) 203–212.
[61] X. Ye, R.A. Kumar, D.J. Patel, Molecular recognition in the bovine immunodeficiency virus Tat peptide-TAR RNA complex, Chem. Biol. 2 (1995) 827–840.
[62] F. Jiang, A. Gorin, W. Hu, A. Majumdar, S. Baskerville, W. Xu, A. Ellington, D.J. Patel, Anchoring an extended HTLV-1 Rex peptide within an RNA major groove containing junctional base triples, Structure 7 (1999) 1461–1472.
[63] Y. Gosser, T. Hermann, A. Majumdar, W. Hu, R. Frederick, F. Jiang, W. Xu, D.J. Patel, Peptide-triggered conformational switch in HIV-1 RRE RNA complexes, Nat. Struct. Mol. Biol. 8 (2001) 146–150.
[64] C. Faber, M. Schärpf, T. Becker, H. Sticht, P. Rösch, The structure of the coliphage HK022 Nun protein-λ-phage boxB RNA complex, J. Biol. Chem. 276 (2001) 32064–32070.
[65] Q. Zhang, K. Harada, H.S. Cho, A.D. Frankel, D.E. Wemmer, Structural characterization of the complex of the Rev response element RNA with a selected peptide, Chem. Biol. 8 (2001) 511–520.
[66] J.D. Puglisi, L. Chen, S. Blanchard, A.D. Frankel, Solution structure of a bovine immunodeficiency virus Tat-TAR peptide-RNA complex, Science 270 (1995) 1200–1203.
[67] C.D. Cilley, J.R. Williamson, Structural mimicry in the phage ϕ21 N peptide–boxB RNA complex, RNA. 9 (2003) 663–676.
[68] V. Calabro, M.D. Daugherty, A.D. Frankel, A single intermolecular contact mediates intramolecular stabilization of both RNA and protein, Proc. Natl Acad. Sci. U.S.A. 102 (2005) 6849–6854.
[69] T.C. Leeper, Z. Athanassiou, R.L. Dias, J.A. Robinson, G. Varani, TAR RNA recognition by a cyclic peptidomimetic of Tat protein, Biochemistry 44 (2005) 12362–12372.
[70] X. Ye, A. Gorin, R. Frederick, W. Hu, A. Majumdar, W. Xu, G. McLendon, A. Ellington, D.J. Patel, RNA architecture dictates the conformations of a bound peptide, Chem. Biol. 6 (1999) 657–669.
[71] M. Schärpf, H. Sticht, K. Schweimer, M. Boehm, S. Hoffmann, P. Rösch, Antitermination in bacteriophage: the structure of the N36 peptide-boxB RNA complex, FEBS J. 267 (2000) 2397–2408.
[72] X. Ye, A. Gorin, A.D. Ellington, D.J. Patel, Deep penetration of an α-helix into a widened RNA major groove in the HIV-1 rev peptide–RNA aptamer complex, Nat. Struct. Mol. Biol. 3 (1996) 1026–1033.
[73] H.M. Berman, T.N. Bhat, P.E. Bourne, Z. Feng, G. Gilliland, H. Weissig, J. Westbrook, The Protein Data Bank and the challenge of structural genomics, Nat. Struct. Mol. Biol. 7 (2000) 957–959.
[74] T.J. Dolinsky, J.E. Nielsen, J.A. McCammon, N.A. Baker, PDB2PQR: an automated pipeline for the setup of Poisson–Boltzmann electrostatics calculations, Nucleic Acids Res. 32 (2004) W665–W667.
[75] T.J. Dolinsky, P. Czodrowski, H. Li, J.E. Nielsen, J.H. Jensen, G. Klebe, N.A. Baker, PDB2PQR: expanding and upgrading automated preparation of biomolecular structures for molecular simulations, Nucleic Acids Res. 35 (2007) W522–W525.
[76] W.D. Cornell, P. Cieplak, C.I. Bayly, I.R. Gould, K.M. Merz, D.M. Ferguson, D.C. Spellmeyer, T. Fox, J.W. Caldwell, P.A. Kollman, A second generation force field for the simulation of proteins, nucleic acids, and organic molecules, J. Am. Chem. Soc. 117 (1995) 5179–5197.
[77] K.A. Sharp, Polyelectrolyte electrostatics: salt dependence, entropic, and enthalpic contributions to free energy in nonlinear Poisson–Boltzmann model, Biopolymers 36 (2005) 227–243.
[78] B.R. Brooks, C.L. Brooks III, A.D. Mackerell Jr., L. Nilsson, R.J. Petrella, B. Roux, Y. Won, G. Archontis, C. Bartels, S. Boresch, L. Caflisch, L. Caves, Q. Cui, A.R. Dinner, M. Feig, S. Fischer, J. Gao, M. Hodoscek, W. Im, K. Kuczera, T. Lazaridis, J. Ma, V. Ovchinnikov, E. Paci, R.W. Pastor, C.B. Post, J.Z. Pu, M. Schaeffer, B. Tidor, R.M. Venable, H.L. Woodcock, X. Wu, W. Yang, D.M. York, M. Karplus, CHARMM: the biomolecular simulation program, J. Comput. Chem. 30 (2009) 1545–1614.
[79] B. Hribar, V. Vlachy, L.B. Bhuiyan, C.W. Outhwaite, Ion distributions in a cylindrical capillary as seen by the modified Poisson–Boltzmann theory and Monte Carlo simulations, J. Phys. Chem. B 104 (2000) 11522–11527.
[80] Y. Levin, Electrostatic correlations: from plasma to biology, Rep. Prog. Phys. 65 (2002) 1577–1632.
[81] R.R. Netz, Electrostatistics of counter-ions at and between planar charged walls: from Poisson–Boltzmann to the strong-coupling theory, Eur. Phys. J. E 5 (2001) 557–574.
[82] R.R. Netz, H. Orland, Field theory for charged fluids and colloids, Europhys. Lett. 45 (1999) 726–732.
[83] R.R. Netz, H. Orland, Beyond Poisson–Boltzmann: fluctuation effects and correlation functions, Eur. Phys. J. E 1 (2000) 203–214.
[84] R. Penfold, S. Nordholm, B. Jönsson, C.E. Woodward, A simple analysis of ion–ion correlation in polyelectrolyte solutions, J. Chem. Phys. 92 (1990) 1915–1922.
[85] Z. Tan, S. Chen, RNA helix stability in mixed Na+/Mg2+ solution, Biophys. J. 92 (2007) 3615–3632.
[86] S. Chen, RNA folding: conformational statistics, folding kinetics, and ion electrostatics, Annu. Rev. Biophys. 37 (2008) 197–214.
[87] M.T. Record Jr., P.L. DeHaseth, T.M. Lohman, Interpretation of monovalent and divalent cation effects on the lac repressor–operator interaction, Biochemistry 16 (1977) 4791–4796.
[88] T.M. Lohman, P.L. DeHaseth, M.T. Record Jr., Pentalysine-deoxyribonucleic acid interactions: a model for the general effects of ion concentrations on the interactions of proteins with nucleic acids, Biochemistry 19 (1980) 3522–3530.
[89] G.S. Manning, J. Ray, Counterion condensation revisited, J. Biomol. Struct. Dyn. 16 (1998) 461–476.